

The Widom line and dynamical crossover in supercritical water: Popular water models versus experiments

D. Corradini, M. Rovere, and P. Gallo

Citation: *The Journal of Chemical Physics* **143**, 114502 (2015); doi: 10.1063/1.4930542

View online: <http://dx.doi.org/10.1063/1.4930542>

View Table of Contents: <http://scitation.aip.org/content/aip/journal/jcp/143/11?ver=pdfcov>

Published by the [AIP Publishing](#)

Articles you may be interested in

[Evidence for structural crossover in the supercritical state](#)

J. Chem. Phys. **139**, 234501 (2013); 10.1063/1.4844135

[The dynamical crossover in attractive colloidal systems](#)

J. Chem. Phys. **139**, 214502 (2013); 10.1063/1.4833595

[Fragile to strong crossover at the Widom line in supercooled aqueous solutions of NaCl](#)

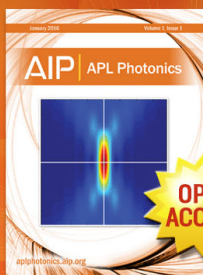
J. Chem. Phys. **139**, 204503 (2013); 10.1063/1.4832382

[Diffusion anomaly and dynamic transitions in the Bell–Lavis water model](#)

J. Chem. Phys. **133**, 104904 (2010); 10.1063/1.3479001

[Dynamic transitions in a two dimensional associating lattice gas model](#)

J. Chem. Phys. **130**, 184902 (2009); 10.1063/1.3129842



Launching in 2016!

The future of applied photonics research is here

**OPEN
ACCESS**

AIP | APL
Photonics

The Widom line and dynamical crossover in supercritical water: Popular water models versus experiments

D. Corradini,^{1,a)} M. Rovere,² and P. Gallo^{2,3,b)}

¹Center for Polymer Studies and Department of Physics, Boston University, 590 Commonwealth Avenue, Boston, Massachusetts 02215, USA

²Dipartimento di Matematica e Fisica, Università Roma Tre, Via della Vasca Navale 84, I-00146 Rome, Italy

³INFN Sez. Roma Tre, Via della Vasca Navale 84, I-00146 Rome, Italy

(Received 14 July 2015; accepted 27 August 2015; published online 15 September 2015)

In a previous study [Gallo *et al.*, Nat. Commun. **5**, 5806 (2014)], we have shown an important connection between thermodynamic and dynamical properties of water in the supercritical region. In particular, by analyzing the experimental viscosity and the diffusion coefficient obtained in simulations performed using the TIP4P/2005 model, we have found that the line of response function maxima in the one phase region, the Widom line, is connected to a crossover from a liquid-like to a gas-like behavior of the transport coefficients. This is in agreement with recent experiments concerning the dynamics of supercritical simple fluids. We here show how different popular water models (TIP4P/2005, TIP4P, SPC/E, TIP5P, and TIP3P) perform in reproducing thermodynamic and dynamic experimental properties in the supercritical region. In particular, the comparison with experiments shows that all the analyzed models are able to qualitatively predict the dynamical crossover from a liquid-like to a gas-like behavior upon crossing the Widom line. Some of the models perform better in reproducing the pressure-temperature slope of the Widom line of supercritical water once a rigid shift of the phase diagram is applied to bring the critical points to coincide with the experimental ones. © 2015 AIP Publishing LLC. [<http://dx.doi.org/10.1063/1.4930542>]

I. INTRODUCTION

The phase diagram of a fluid shows a region where at given pressure P and temperature T two coexisting phases, gas and liquid, are present separated by the gas-liquid coexisting line. This line terminates at the critical point (T_c , P_c). In the supercritical region ($P > P_c$ and $T > T_c$), the system goes in a single fluid phase.

Supercritical fluids are of great interest in many applied and fundamental fields of research. In particular, supercritical water attracts industrial interest as a medium for extraction of coal, for waste disposal, biomass liquefaction, and for being important in many geochemical processes.^{1–3} It has been recently found that in supercritical water different regimes are still present although they are not separated by any first order line of transition as in the subcritical region. In particular, a dynamical crossover for the viscosity has been found, with a change from gas-like to a liquid-like behavior.⁴ The crossover between the two regimes takes place by crossing the Widom line, the line that connects the maxima of the thermodynamic response functions upon approaching the critical point from the single supercritical phase.^{5–9}

This appears to be in analogy with the crossover found in the dynamics of supercooled water at the crossing of the

Widom line associated with the presence of a possible liquid-liquid critical point.^{10–26}

In the region of the gas-liquid transition, it is generally observed that departing from the critical point and entering into the supercritical region the maxima of the response functions progressively weaken. The range of definition of the Widom line is particularly relevant for water since it is equivalent to the range where the peculiar properties of supercritical water are evidenced.²⁷

From the theoretical point of view, a great progress in the comprehension of water properties is due to computer simulation. There are now a number of site models that are simple enough to be used also for large scale simulations and that are able to reproduce the main features of water in large portions of the thermodynamic space in some cases with shifts in pressure and/or temperature.^{28,29} Some of the rigid site models for water, like SPC/E,³⁰ TIP4P,³¹ and the more recent TIP4P/2005^{17,28} have been shown to give good predictions for the thermodynamic properties of supercritical water³² and also good predictions for the critical point of water.

In order to get more insight into the unusual properties of supercritical water, it is of great interest to look more in detail at the general predictions of those theoretical models and compare these predictions with experiments.

In this paper, we consider how different models of water predict the thermodynamic and dynamical quantities that characterize supercritical water in order to get a better understanding of their ability in reproducing the phenomenology of water under such extreme conditions of pressures and temperatures. In particular, we will compare the slope of the

^{a)}Present address: Laboratoire PASTEUR, UMR 8640 ENS-CNRS-UPMC Paris 6, Département de Chimie, École Normale Supérieure, 75005 Paris, France.

^{b)}Author to whom correspondence should be addressed. Electronic mail: gallop@fis.uniroma3.it

Widom line with the experimental results due to the relevance of that curve in understanding the properties of supercritical water.

The models that we considered are widely used in the literature and they are TIP4P/2005;³³ TIP4P;³¹ SPC/E;³⁰ TIP5P;³⁴ and TIP3P.³¹

We compare the phenomenology that we derived from the simulations of thermodynamic and diffusion properties with the experimental results taken from NIST Chemistry Web-book website.³⁵

The paper is structured as follows. In Sec. II, we describe the simulation methods and the water models. In Sec. III, we present the results of the calculations of the Widom line as derived from the maxima of the thermodynamic response functions both in simulations and in experiments. In Sec. IV, we consider the behavior of the experimental viscosity and of the simulated diffusion coefficients in the supercritical region. Sec. V is devoted to conclusions.

II. WATER MODELS AND SIMULATION METHODS

We perform molecular dynamics simulations using five different rigid site models for water, namely TIP4P/2005;³³ TIP4P;³¹ SPC/E;³⁰ TIP5P;³⁴ and TIP3P.³¹

We recall that all the models represent the water molecule as a rigid system with three (SPC/E and TIP3P) or four (TIP4P and TIP4P/2005) or five (TIP5P) sites. These potentials are modeled with a Lennard-Jones interaction between the oxygen sites and a Coulombic interaction between the charged sites.

The interaction potentials can therefore be written as follows:

$$U(r_{ij}) = 4\epsilon_{ij} \left[\left(\frac{\sigma_{ij}}{r_{ij}} \right)^{12} - \left(\frac{\sigma_{ij}}{r_{ij}} \right)^6 \right] + \frac{q_i q_j}{r_{ij}}, \quad (1)$$

where r_{ij} is the distance between two interacting sites, q_i is the charge of a water site, and ϵ_{ij} is different from zero only for the oxygen sites.

A positive charge is assigned to the hydrogen sites in all the models. In the three site systems, the oxygen has a negative charge, while in TIP4P and TIP4P/2005, the oxygen site is neutral and the negative charge is shifted to a dummy site close to oxygen site. In TIP5P to represent the lone pair of the water oxygen the negative charge is carried by two dummy sites. The geometrical and interaction parameters of the models are reported in Table I.

The simulations have been performed in a cubic box containing 4096 water molecules with an initial density $\rho = 1.0 \text{ g/cm}^3$. We investigated pressures above the liquid-gas critical pressure for each model. The critical parameters of the different models are reported in Table II. Starting from $P = P_c + 25 \text{ bars}$, the simulations have been performed at ten different pressures with $\Delta P = 25 \text{ bars}$. For the temperatures we considered a window of 200 K around the critical temperature with $\Delta T = 5 \text{ K}$. Our isobars never cross the liquid-gas first-order phase transition line.

We performed the simulations using the software GROMACS (versions 4.5.3 and 4.5.5).³⁶ The simulations

TABLE I. Parameters of the model potentials used in this paper. d_{OH} is the distance between the oxygen and the hydrogen sites. H–O–H denotes the angle between the O–H bonds in the molecular plane. σ and ϵ are the parameters of the oxygen-oxygen Lennard-Jones potential, see Eq. (1). With q_H we indicate the positive charge of the hydrogen site. For SPC/E and TIP3P, the negative charge is placed on the oxygen site, while for TIP4P and TIP4P/2005, the negative charge is displaced on a massless point M at distance d_{OM} from the oxygen. For TIP5P, the negative charge is distributed on two lone pair sites at distance d_{OM} from the oxygen site.

| Model | d_{OH} (nm) | H–O–H (°) | σ (nm) | ϵ/k_B (K) | q_H (e) | d_{OM} (nm) |
|------------|------------------|--------------|------------------|-----------------------|--------------|------------------|
| SPC/E | 0.1 | 109.47 | 0.31656 | 78.20 | 0.423 | 0 |
| TIP3P | 0.09572 | 104.52 | 0.31506 | 76.54 | 0.417 | 0 |
| TIP4P | 0.09572 | 104.52 | 0.31540 | 78.02 | 0.520 | 0.015 |
| TIP4P/2005 | 0.09572 | 104.52 | 0.31589 | 93.20 | 0.5564 | 0.01546 |
| TIP5P | 0.09572 | 104.52 | 0.31200 | 80.51 | 0.241 | 0.070 |

were run in the NPT ensemble, using the Nose-Hoover thermostat^{37–39} and the Parrinello-Rahman barostat.^{40,41} At all temperatures the duration of equilibration run was of 0.1 ns and the duration of the production run of 1 ns. We simulated in total 2050 different thermodynamic points (considering T , P and specific water model). The total simulation time thus amounts to 2225 ns. This required about 45 000 CPU hours, that correspond to about 62.5 months (i.e., 5.2 yr) when running the simulations on a single core.

The equations of motions were integrated using the leap-frog algorithm with an integration time step of 1 fs. The water molecules were kept rigid by using the SETTLE algorithm,⁴² while the position(s) of the virtual site(s) were recalculated at each time step. We cutoff the short-range interactions at 1 nm and we employed the particle mesh Ewald algorithm to deal with electrostatic interactions.

We extract the oxygen self diffusion coefficient from the mean square displacement by using the Einstein relation. For the calculation of the diffusion coefficient, the first and the last 10% of the run are excluded from the linear fit of the mean square displacement.

III. WIDOM LINE OF THE LIQUID-GAS TRANSITION

Table II summarizes the critical values (T_C, P_C, ρ_C) for experimental water and for the water models taken into consideration in the present work. The parameters reported in Table II indicate that TIP4P/2005 provides the closest critical

TABLE II. Values for the critical parameters from experiments³⁵ compared with the values obtained in computer simulations and taken from Ref. 43, original references can be found therein.

| System | T_C (K) | P_C (bars) | ρ_C (g/cm ³) |
|------------|-----------|--------------|-------------------------------|
| Expt. | 647.096 | 220.640 | 0.322 |
| TIP4P/2005 | 640 | 146 | 0.31 |
| TIP4P | 588 | 149 | 0.315 |
| SPC/E | 638.6 | 139 | 0.273 |
| TIP5P | 521 | 86 | 0.337 |
| TIP3P | 578 | 126 | 0.272 |

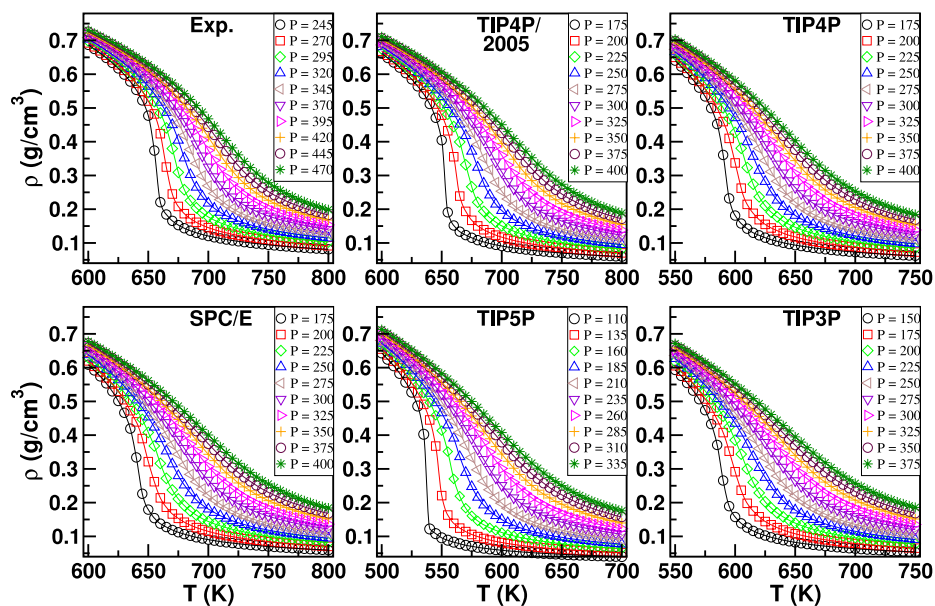


FIG. 1. Isobars of supercritical water from experiments³⁵ and calculated with the water models: TIP4P/2005; TIP4P; SPC/E; TIP5P; TIP3P. Pressures are in bar.

temperature and density with respect to the experimental findings. TIP4P has a shift of around 70 K in T_C with a good value for the critical density. We note that all the models fail to reproduce the experimental critical pressure. For TIP4P/2005 and TIP4P, the difference is of the order of 30% but it increases to 60% for the TIP5P model.

In Fig. 1, we present the isobars of water in the supercritical region as calculated from our simulations for the five different water models and compared with the experimental isobars.³⁵ As explained in Sec. II in each case the isobars are calculated for values of T and P at approximately the same distance from the respective critical values. The curves show the expected behavior of a fluid approaching the critical point. The envelope of the TIP4P/2005 isobars appears to be the closest to the experimental case but also the TIP4P model reproduces quite well the experimental behavior if the shift of approximately 70 K in temperature is considered.

In order to more quantitatively assess the agreement between simulations and experiments we did plot in Fig. 2 the isobars obtained with the simulations each one superposed to the experimental isobars as function of the scaled variables $T - T_C$ and $\rho - \rho_C$. In Fig. 3 similarly, the isobars of the models are shifted in such way that their ρ_c coincides with that of experimental water and they are compared with experimental isobars. We can see from these figures that TIP4P/2005 and TIP4P perform remarkably well in reproducing the envelope of the experimental isobars. SPC/E is also rather good but deviations start to appear especially in the gas portion of the curves. TIP3P and TIP5P are the least performing models, since evident deviations from the experimental behavior are observed.

In order to locate the Widom line in the pressure-temperature (PT) plane we calculated from simulations and extracted from experimental data the maxima of the constant

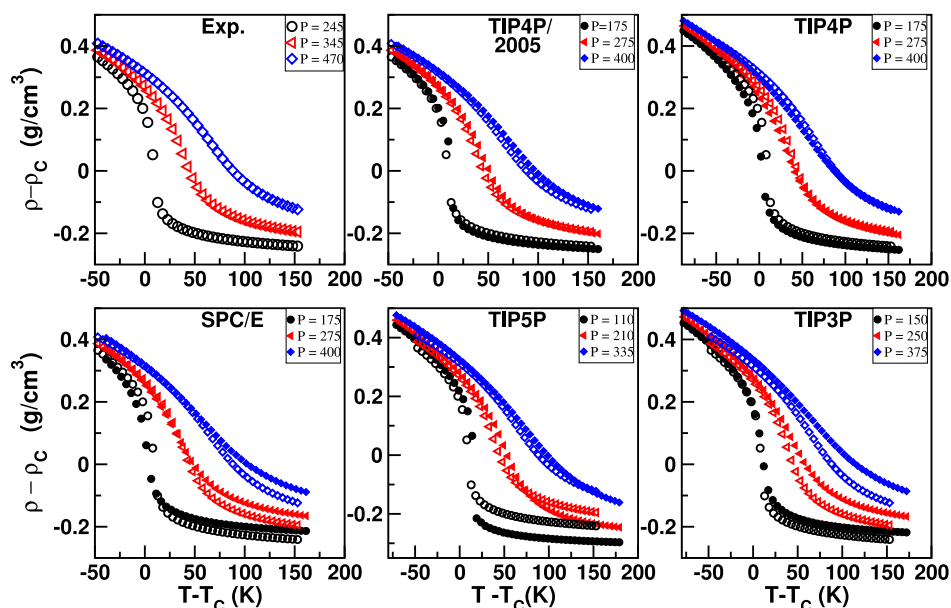


FIG. 2. A direct comparison between isobars calculated with the water models: TIP4P/2005; TIP4P; SPC/E; TIP5P; TIP3P and experimental data³⁵ are shown in this figure by shifting the temperatures and densities of the isobars. Open symbols are experimental lines and full symbols are simulation results from the models.

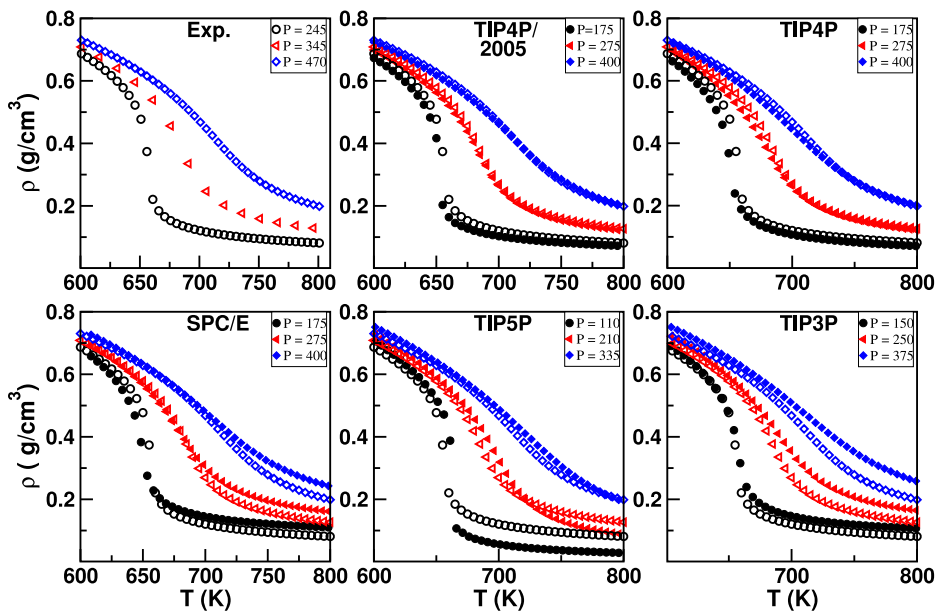


FIG. 3. A comparison between isobars calculated with the water models: TIP4P/2005; TIP4P; SCP/E; TIP5P; TIP3P and experimental data³⁵ is shown in this figure by shifting the isobars of the models so that their ρ_c coincides with that of experimental water. Open symbols are experimental lines and full symbols are simulations results from the models.

pressure specific heat C_P (not shown) defined as

$$C_P = \frac{1}{N} \left(\frac{\partial H}{\partial T} \right)_P, \quad (2)$$

where H is the enthalpy, the maxima of the coefficient of thermal expansion α_P ,

$$\alpha_P = -\frac{1}{\rho} \left(\frac{\partial \rho}{\partial T} \right)_P \quad (3)$$

and the maxima of the isothermal compressibility,

$$K_T = \frac{1}{\rho} \left(\frac{\partial \rho}{\partial P} \right)_T. \quad (4)$$

We report and compare the results obtained in Fig. 4. We observe that in the experiment the lines of the maxima of C_P and α_P are almost coincident for all the range of temperatures

and pressures investigated while the line of K_T maxima merges with the others only upon approaching the critical point. The deviation of the line of K_T maxima from the other lines occurs at $T \approx T_c + 30$ K. The same trend is found in the simulations of all models. In fact, at a given distance from the critical point, the line of K_T maxima is also separated from the lines of C_P and α_P maxima that instead remain very close to each other in the whole span investigated. Moreover, the line of K_T maxima of experimental water and in TIP4P/2005 starts to deviate from C_P and α_P around $T > 1.05 T_c$ and $P > 1.4 P_c$. This deviation takes place closer to the critical coordinates in the simulations of the other models, especially TIP3P.

Similar effects were found in simulations of Lennard-Jones fluids²⁷ but in our case the C_P and the α_P almost coincide in all the range explored.

Apart from the differences in the position in the thermodynamic plane due to the different location of the critical point for each water model, we note that the slope of the Widom line of TIP4P, SPC/E, and TIP4P/2005 is more similar to the experimental one, while the TIP5P and TIP3P curves deviate from the correct slope in approaching the critical point.

In order to better compare the experimental Widom line with the Widom line obtained from simulations, the curves are shown in Fig. 5 where we rigidly shifted the different Widom lines (from maxima of C_P) by values of $\Delta P = P - P_c$ and $\Delta T = T - T_c$ for each model. It is evident that TIP4P, TIP4P/2005, and SPC/E show a better agreement with the experiment, while for TIP5P and TIP3P, the discrepancy with the experiment is larger and it cannot be retrieved by a rigid shift in the thermodynamic space.

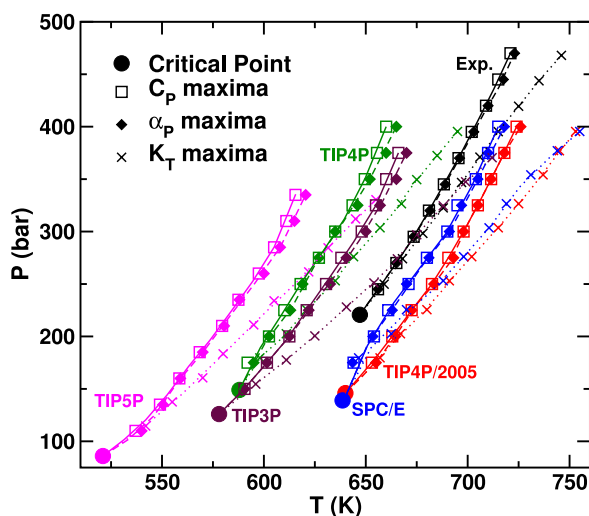


FIG. 4. Critical points and (P, T) locations of C_P , α_P , and K_T maxima from experiments³⁵ and from the calculations with the water models TIP4P/2005; TIP4P; SCP/E; TIP5P; TIP3P. The thermodynamic response function are defined in the text. K_T maxima are calculated along isobars.

IV. DIFFUSION PROPERTIES IN THE SUPERCRITICAL REGION

We consider now the diffusion properties in the supercritical region. We concentrate on the mobility of oxygens in water.

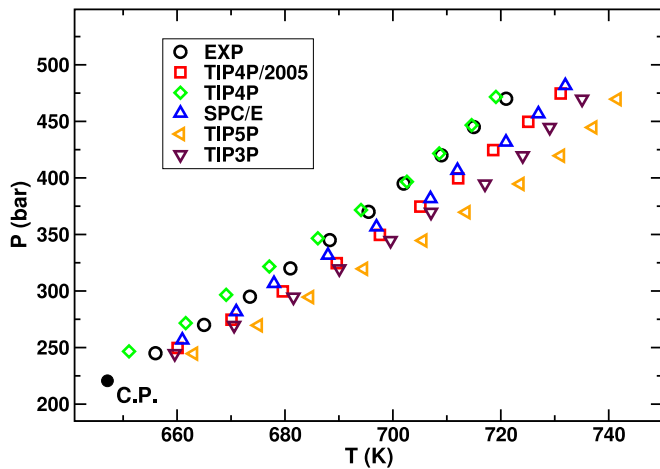


FIG. 5. Maxima of C_P assumed as proxy for the Widom line. The results of the simulation are shifted in pressure and temperature to match the critical coordinates of experimental water. The shifts in pressure and temperature are $\Delta P = 134.64$ bars and $\Delta T = 126.069$ K for TIP5P, $\Delta P = 94.64$ bars and $\Delta T = 69.069$ K for TIP3P, $\Delta P = 71.64$ bars and $\Delta T = 59.096$ K for TIP4P; $\Delta P = 74.64$ bars with $\Delta T = 7.096$ K for TIP4P/2005 and $\Delta P = 81.64$ bars with $\Delta T = 8.50$ K for SPC/E.

Experimental results for water viscosity η in the supercritical region are reported in Fig. 6 together with the inverse of the diffusion coefficients D calculated with the different models. On approaching the critical pressure from the one phase region, the curves of η show an almost vertical change with temperature. The inverse of diffusion coefficient behaves similarly. All the curves remain continuous as expected in the supercritical region but at the lower pressures they show a strong change of slope. In the same figure, we explicitly mark the values of η or D^{-1} extrapolated at the P and T values of the Widom line defined in Sec. III from the maxima of the isobaric specific heat.

As already observed in our previous paper,⁴ we found the interesting result that the Widom line signs a change of behavior of the viscosity in experiments and of the diffusion in simulations from a liquid-like to a gas-like in going from

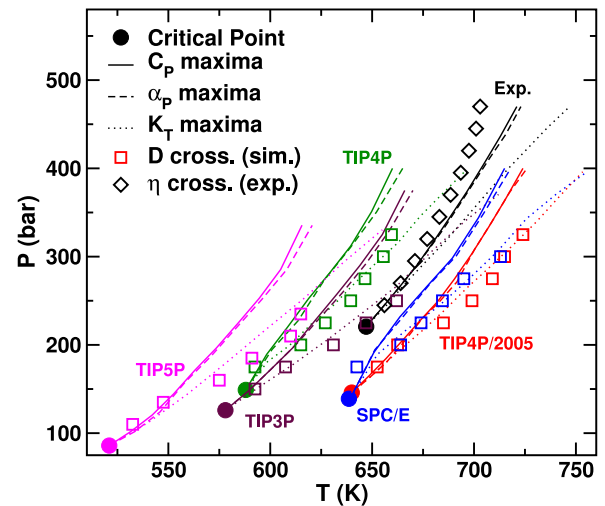


FIG. 7. (P, T) location of viscosity crossovers for experiments;³⁵ (P, T) location of diffusion coefficient crossovers for TIP4P/2005; TIP4P; SPC/E; TIP5P; TIP3P. The crossover points are compared with the lines of maxima of the thermodynamic response functions discussed earlier, see Fig. 4.

high pressures and low temperatures to low pressures and high temperatures.

The behavior of the experimental viscosity above the Widom line shows a monotonic decrease upon increasing T for each pressure, while upon crossing the Widom line the viscosity starts to increase with temperature for low enough pressures, a typical gas-like behavior.⁴⁴ Furthermore, we have shown⁴ that the viscosity in the extreme low pressure range is well fitted by a formula valid in the dilute gas limit.⁴⁵

The diffusion coefficients of the different models of water show as well a change of slope in crossing the Widom line. This change of trend is related to a decrease in the activation energy for increasing temperature as shown in detail in our previous work for the TIP4P/2005 model.⁴

In order to locate more precisely the inflection points of the transport coefficients we calculated the numerical derivatives of the curves. The results are reported in Fig. 7, where we

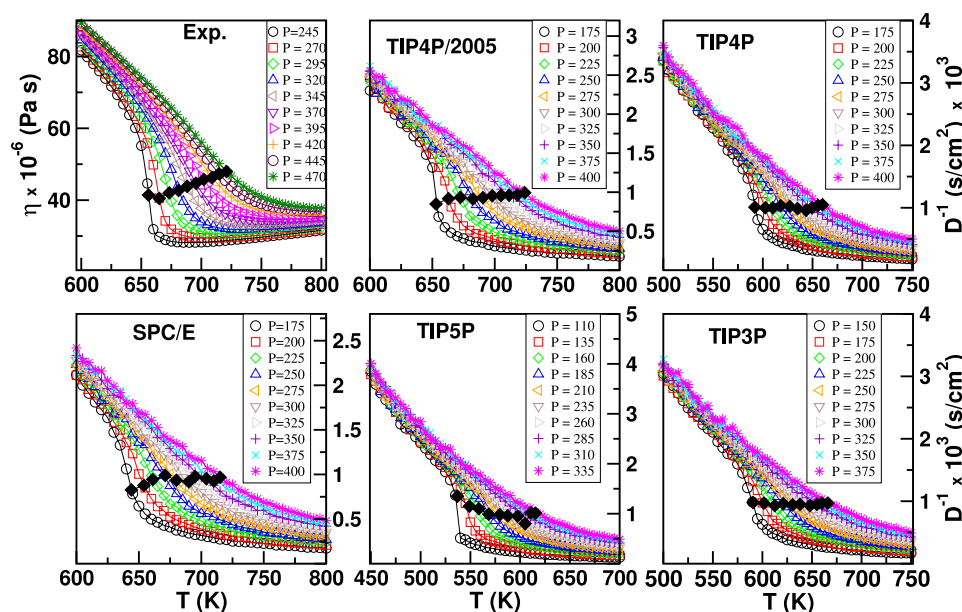


FIG. 6. Viscosity from experiments³⁵ and the inverse of the diffusion coefficient for the different water models, as indicated, at supercritical conditions. In each panel, the extrapolation of η or D^{-1} at the P and T values of the Widom line (black diamonds) is reported. Pressures are in bar.

compare them with the Widom line obtained with the different criteria.

Looking at Fig. 7, it is evident that the lines of the viscosity and the diffusion coefficient crossovers located through the derivatives coincide with the Widom line only upon approaching the critical point. In particular we note that the line of crossover of the experimental viscosity follows the Widom line for almost 30 K and its deviation toward low T is less strong with respect to the numerical models. In the simulations, the lines of the diffusion coefficient crossovers deviate downwards from the Widom line sooner after the critical point at variance with the upwards deviation of the viscosity crossover. This is a common feature of all the models considered.

Nonetheless in spite of the differences, all the models show the strict relation between the Widom line and the transport properties.

V. CONCLUSIONS

We considered the thermodynamic properties of water along the isobars in the supercritical region by comparing the experimental data with simulation results obtained from different rigid site models for water. We calculated in each case the lines of the maxima of C_P , K_T and α_P in the single phase region above the critical point. These curves are related to the Widom line, defined as the line of the maxima of the correlation length. Starting from (T_C, P_C) by varying the temperature at constant pressure we find that the curves of the C_P and α_P maxima follow a similar path, while the maxima of K_T deviates from the other two lines at some distance from the critical point. Nevertheless, a Widom line is clearly discernible for experimental water and all water models, at least in the range where the lines of maxima of the three response functions considered all coincide. Among the water models TIP4P/2005, TIP4P, and SPC/E show the best agreement with the experiments in the prediction of the Widom line.

We also found interesting results for the experimental viscosity and for the diffusion coefficients obtained in simulations. We observed that upon crossing the Widom line there is a crossover from a liquid-like to a gas-like behavior. In this way, it is possible to associate to this crossover the presence of further lines associated to the Widom line. These findings are in agreement with recent experimental results on the crossover of dynamical properties across the Widom line in supercritical fluids.^{46,47} In noble gases another line, the Frenkel line has also been used to characterize region of different dynamical behaviour in the supercritical state.^{48,49} Crossover of thermodynamic and structural properties in supercritical water has been also interpreted in terms of a percolation transition see Refs. 50 and 51 and references therein. Moreover, it is interesting to note that the Widom line marks the crossover between different dynamical regimes of water also in the region of the supercooled liquid.^{10,19,52} This is a clear indication of how important is the Widom line to understand the connection between the thermodynamic properties and the dynamical behavior. Since the role of the Widom line appears so relevant

it would be of great interest in future work to extend the present study to other fluids in the supercritical region.

ACKNOWLEDGMENTS

We gratefully acknowledge the computational support of the Roma Tre INFN-GRID.

- ¹C. Aymonier, A. Loppinet-Seran, H. Reveron, Y. Garrabos, and F. Cansell, *J. Supercrit. Fluids* **38**, 242 (2006).
- ²T. Adschiri, Y. W. Lee, M. Goto, and S. Takami, *Green Chem.* **13**, 1380 (2011).
- ³C. M. Huelsman and P. E. Savage, *J. Supercrit. Fluids* **81**, 200 (2013).
- ⁴P. Gallo, D. Corradini, and M. Rovere, *Nat. Commun.* **5**, 5806 (2014).
- ⁵P. F. McMillan and H. E. Stanley, *Nat. Phys.* **6**, 479 (2010).
- ⁶G. Franzese and H. E. Stanley, *J. Phys.: Condens. Matter* **19**, 205126 (2007).
- ⁷G. Ruppeiner, A. Sahay, T. Sarkar, and G. Sengupta, *Phys. Rev. E* **86**, 052103 (2012).
- ⁸V. V. Brazhkin, Y. D. Fomin, V. N. Ryzhov, E. E. Tareyeva, and E. N. Tsiok, *Phys. Rev. E* **89**, 042136 (2014).
- ⁹H. O. May, P. Mausbach, and G. Ruppeiner, *Phys. Rev. E* **91**, 032141 (2015).
- ¹⁰L. Xu, P. Kumar, S. V. Buldyrev, S.-H. Chen, P. H. Poole, F. Sciortino, and H. E. Stanley, *Proc. Natl. Acad. Sci. U. S. A.* **102**, 16558 (2005).
- ¹¹L. Liu, S.-H. Chen, A. Faraone, C.-W. Yen, and C.-Y. Mou, *Phys. Rev. Lett.* **95**, 117802 (2005).
- ¹²L. Xu, S. V. Buldyrev, C. Angell, and H. Stanley, *Phys. Rev. E* **74**, 031108 (2006).
- ¹³D. Fuentesvella and M. Anisimov, *Phys. Rev. Lett.* **97**, 195702 (2006).
- ¹⁴F. Mallamace, M. Broccio, C. Corsaro, A. Faraone, D. Majolino, V. Venuti, L. Liu, C.-Y. Mou, and S.-H. Chen, *Proc. Natl. Acad. Sci. U. S. A.* **104**, 424 (2007).
- ¹⁵C. Huang, K. T. Wikfeldt, T. Tokushima, D. Nordlund, Y. Harada, U. Bergmann, M. Niebuhr, T. Weiss, Y. Horikawa, M. Leetmaa, M. P. Ljungberg, O. Takahashi, A. Lenz, L. Ojamae, A. P. Lyubartsev, S. Shin, L. G. M. Pettersson, and A. Nilsson, *Proc. Natl. Acad. Sci. U. S. A.* **106**, 15214 (2009).
- ¹⁶D. Banerjee, S. N. Bhat, S. V. Bhat, and D. Leporini, *Proc. Natl. Acad. Sci. U. S. A.* **106**, 11448 (2009).
- ¹⁷J. L. F. Abascal and C. Vega, *J. Chem. Phys.* **133**, 234502 (2010).
- ¹⁸K. T. Wikfeldt, C. Huang, A. Nilsson, and L. G. M. Pettersson, *J. Chem. Phys.* **134**, 214506 (2011).
- ¹⁹P. Gallo and M. Rovere, *J. Chem. Phys.* **137**, 164503 (2012).
- ²⁰D. Corradini, P. Gallo, S. V. Buldyrev, and H. Stanley, *Phys. Rev. E* **85**, 051503 (2012).
- ²¹P. Gallo, D. Corradini, and M. Rovere, *J. Chem. Phys.* **139**, 204503 (2013).
- ²²E. Salcedo, N. Barraz, and M. Barbosa, *J. Chem. Phys.* **118**, 164502 (2013).
- ²³J. Luo, L. Xu, E. Lascaris, H. E. Stanley, and S. V. Buldyrev, *Phys. Rev. Lett.* **112**, 135701 (2014).
- ²⁴G. Pallares, M. M. Azouzi, M. A. Gonzalez, J. L. Aragonés, J. L. F. Abascal, C. Valeriani, and F. Caupin, *Proc. Natl. Acad. Sci. U. S. A.* **111**, 7936 (2014).
- ²⁵P. Gallo and M. Rovere, *Phys. Rev. E* **91**, 012107 (2015).
- ²⁶C. Buhariwalla, R. Bowles, I. Saika-Voivod, F. Sciortino, and P. Poole, *Eur. Phys. J. E* **38**, 39 (2015).
- ²⁷V. V. Brazhkin, Y. D. Fomin, A. G. Lyapin, V. N. Ryzhov, and E. N. Tsiok, *J. Phys. Chem. B* **115**, 14112 (2011).
- ²⁸C. Vega, J. L. F. Abascal, M. M. Conde, and J. L. Aragonés, *Faraday Discuss.* **141**, 251 (2009).
- ²⁹D. Corradini, M. Rovere, and P. Gallo, *J. Chem. Phys.* **132**, 134508 (2010).
- ³⁰H. J. C. Berendsen, J. R. Grigera, and T. P. Straatsma, *J. Phys. Chem.* **91**, 6269 (1987).
- ³¹W. L. Jorgensen, J. Chandrasekhar, J. D. Madura, R. W. Impey, and M. L. Klein, *J. Chem. Phys.* **79**, 926 (1983).
- ³²P. Jedlovsky and J. Richardi, *J. Chem. Phys.* **110**, 8019 (1999).
- ³³J. L. F. Abascal and C. Vega, *J. Chem. Phys.* **123**, 234505 (2005).
- ³⁴M. W. Mahoney and W. L. Jorgensen, *J. Chem. Phys.* **112**, 8910 (2000).
- ³⁵See <http://webbook.nist.gov/chemistry/fluid/> for *NIST Chemistry WebBook*.
- ³⁶B. Hess, C. Kutzner, D. van der Spoel, and E. Lindahl, *J. Chem. Theory Comput.* **4**, 435 (2008).
- ³⁷S. Nosé, *Mol. Phys.* **52**, 255 (1984).
- ³⁸S. Nosé, *J. Chem. Phys.* **81**, 511 (1984).
- ³⁹W. G. Hoover, *Phys. Rev. A* **31**, 1695 (1985).
- ⁴⁰M. Parrinello and A. Rahman, *J. Appl. Phys.* **52**, 7182 (1981).

- ⁴¹S. Nosé and M. L. Klein, *Mol. Phys.* **50**, 1055 (1983).
- ⁴²S. Miyamoto and P. Kollman, *J. Comput. Chem.* **13**, 952 (1992).
- ⁴³C. Vega and J. L. F. Abascal, *Phys. Chem. Chem. Phys.* **13**, 19663 (2011).
- ⁴⁴S. Chapman and T. G. Cowling, *The Mathematical Theory of Non-Uniform Gases*, 3rd ed. (Cambridge Mathematical Library, Cambridge University Press, 1970).
- ⁴⁵J. V. Sengers, R. A. Perkins, M. L. Huber, and D. G. Friend, *Int. J. Thermophys.* **30**, 374 (2009).
- ⁴⁶F. A. Gorelli, T. Bryk, M. Krisch, G. Ruocco, M. Santoro, and T. Scopigno, *Sci. Rep.* **3**, 1203 (2013).
- ⁴⁷G. G. Simeoni, T. Bryk, F. A. Gorelli, M. Krisch, G. Ruocco, M. Santoro, and T. Scopigno, *Nat. Phys.* **6**, 503 (2010).
- ⁴⁸V. V. Brazhkin, Y. D. Fomin, A. G. Lyapin, V. N. Ryzhov, and K. Trachenko, *Phys. Rev. E* **85**, 031203 (2012).
- ⁴⁹V. V. Brazhkin, Y. D. Fomin, A. G. Lyapin, V. N. Ryzhov, E. N. Tsiok, and K. Trachenko, *Phys. Rev. Lett.* **111**, 145901 (2013).
- ⁵⁰L. Partay and P. Jedlovsky, *J. Chem. Phys.* **123**, 024502 (2005).
- ⁵¹L. V. Woodcock, *J. Phys. Chem. B* **116**, 3735 (2012).
- ⁵²K. T. Wikfeldt, A. Nilsson, and L. G. M. Pettersson, *Phys. Chem. Chem. Phys.* **13**, 19918 (2011).